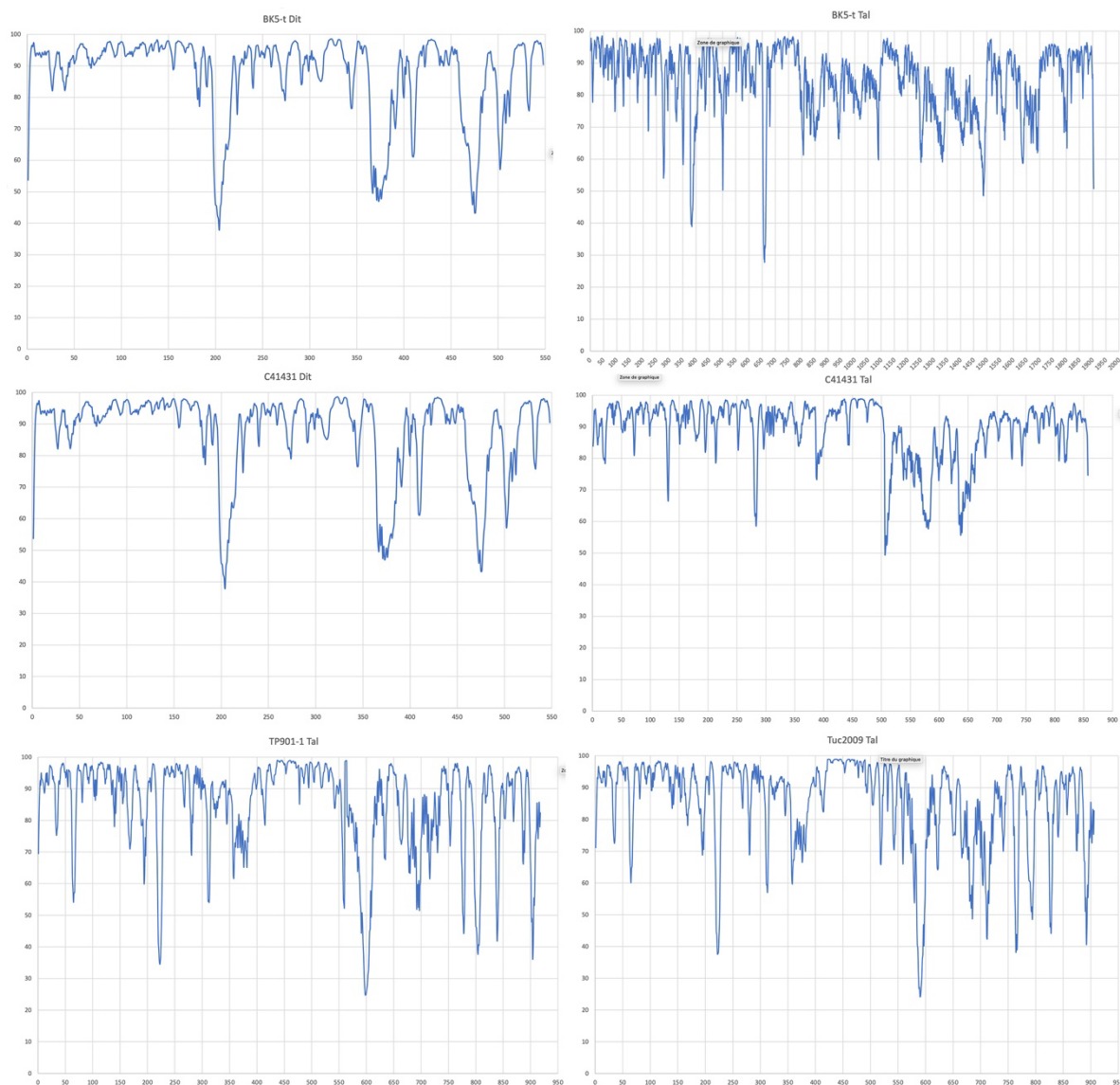
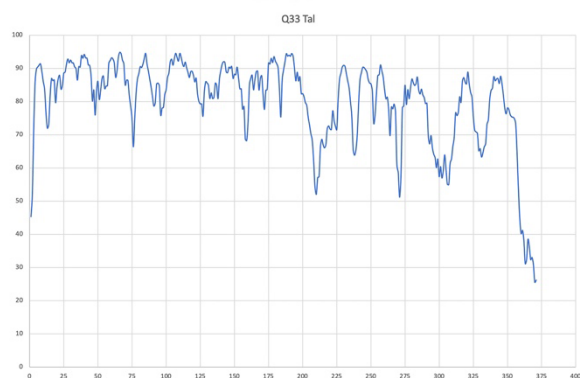
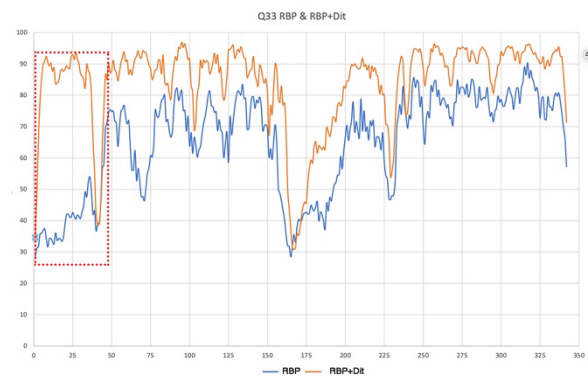
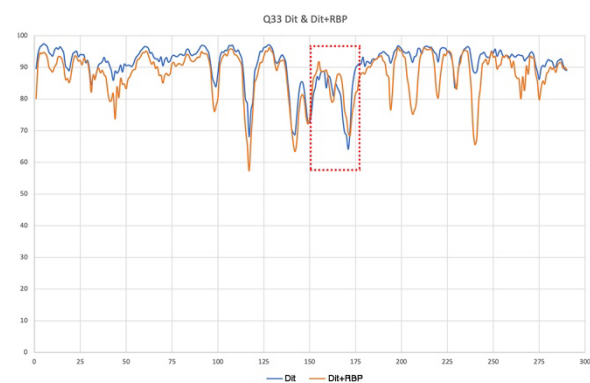
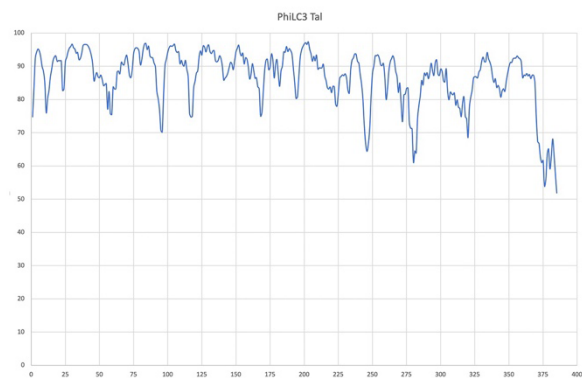
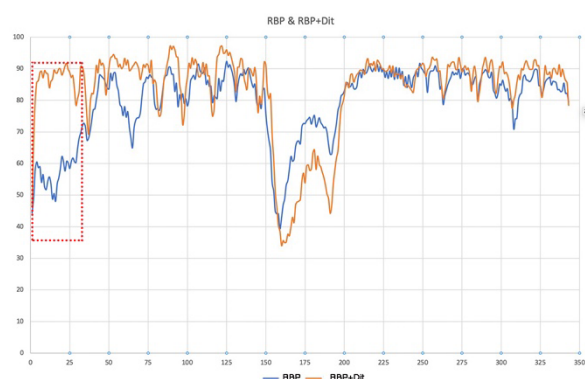
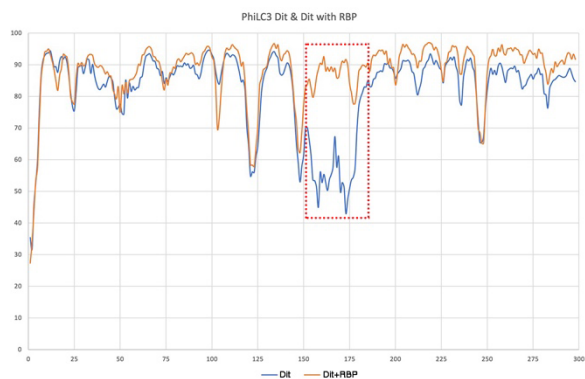


Supplementary Figure S1. Plots of the pLDDT values (y-axis) *vs* the protein sequence (x-axis). (A) Structure predictions of proteins from P335 phages types I and II. **(B)** Structure predictions of proteins from P335 phages types III and IV. The red dots squares identify the Dit arm-hand domain interacting with the RBP N-terminal domain. **(C)** Structure predictions of the NPS proteins from phages PhiLC3, TP901-1 and Tuc2009.

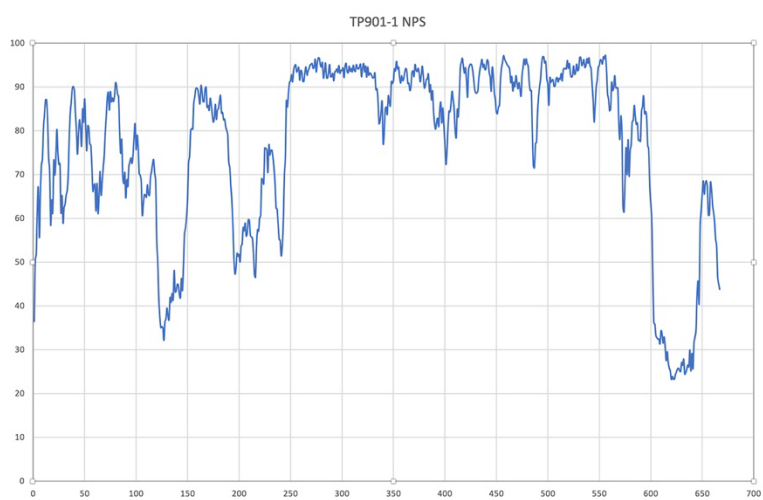
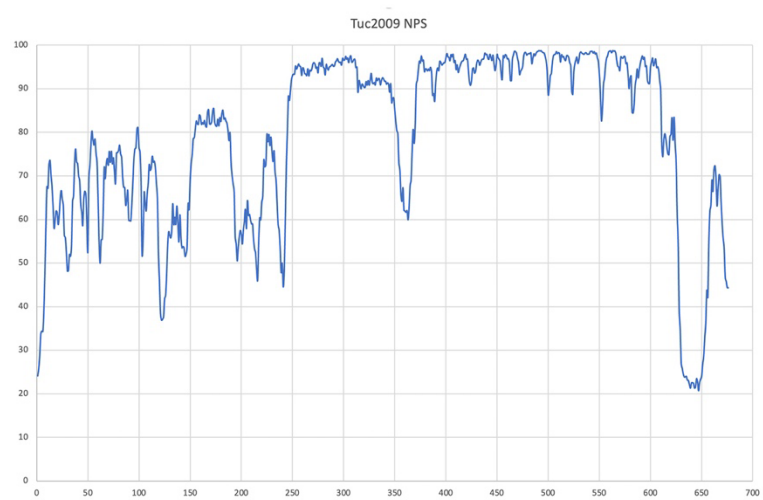
A



B



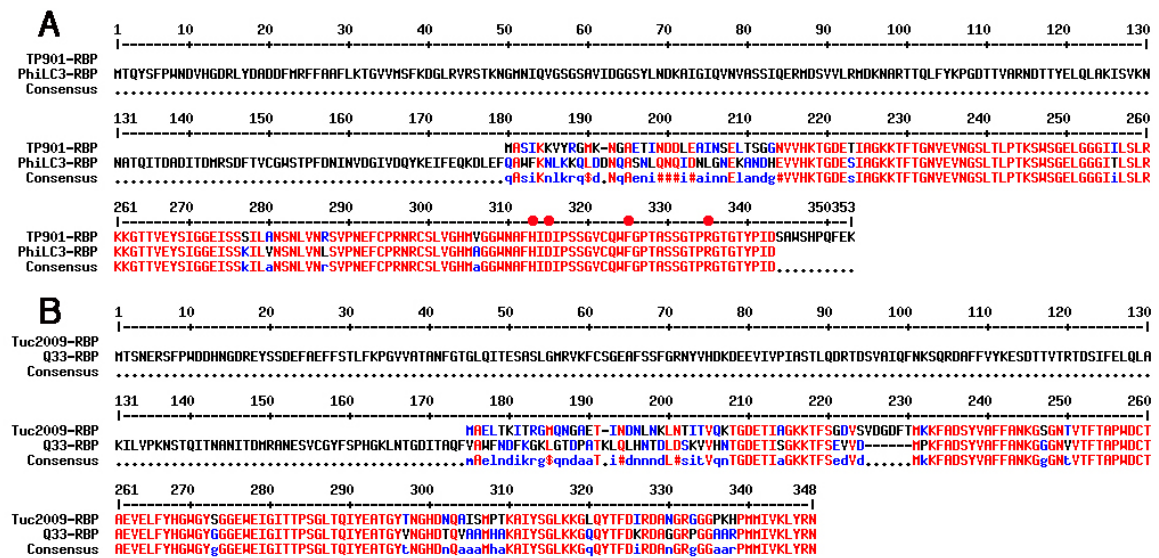
C



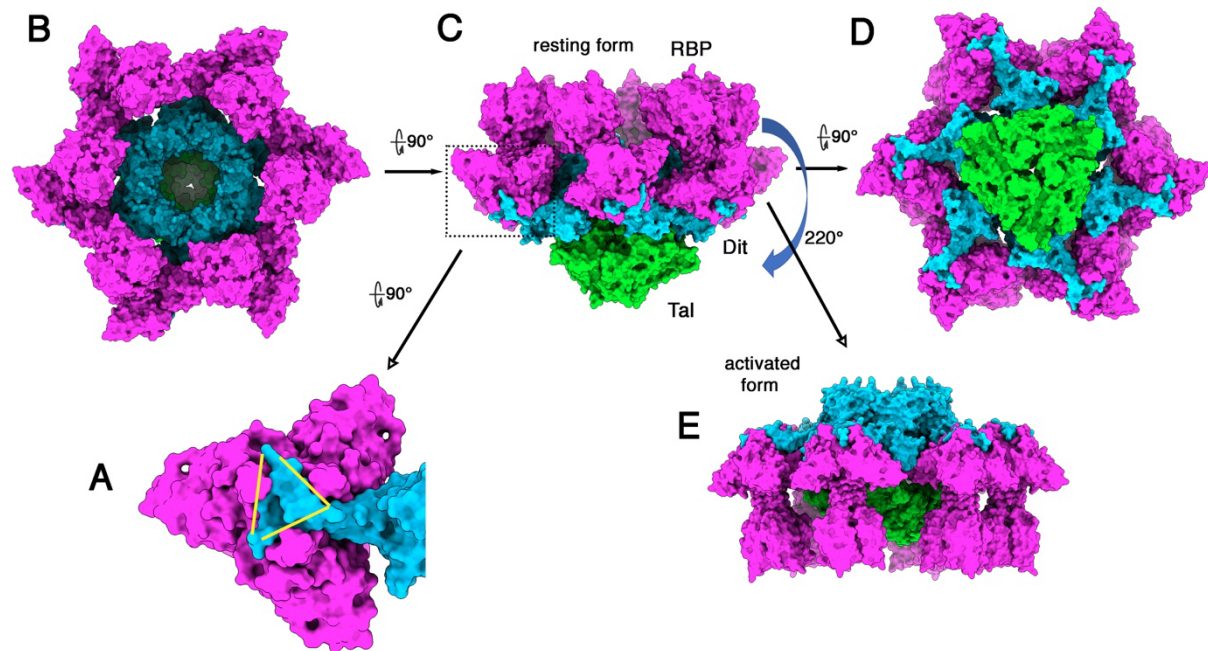
RBP

	1	10	20	30	40	50	60	70	80	90	100	110	120	130
TP901-RBP	HRSIKITVYRHKNGAETITNDOLERINSELTSGGNVVHKTGDETIAGKKKTFIGNVYVNSGLTLPKSHSGELGGGTLILRKKGTITVEYSIGGEISSTLHAGMSNLVNSVPVMEFCPRNRSL--VGHVIVGG													
Tuc2009-RBP	HAEIKTITVYRHKNGAETITNDOLNKLITL-----TVQKTGDETIAGKKTFSGDVSVDGDTFKKFKDYSVYVFFKNGSNTVITFAPMDCITAEVLVFLYGLNSIGGTTGPRKLTQYEAETGYTNG													
Consensus	HReIkK T LRgHkNGAETITNDL#aiNsE.....tVqKTGDETIAGKKTFsG#eYVgdlT k kkadSgeagganigSgrkkgfTaeudcgaE elfihangnlgnrseinefITTSrRqci...aggntnG													
	131	140	150	160	170	179								
TP901-RBP	HNAFHIDIPS---SGVCMQFGPTASSGTPRGGTITYPIDASHNPQFEK													
Tuc2009-RBP	HDNQASIMPTKAIISGLKKGLQYTFDIRDANGGGGKPHMHIKLYRN													
Consensus	h#aqaIdiPs.....SGLeqglapIdardirGrGggPidpanihkq#rn													

Supplementary Figure S3. Sequence alignment of RBP sequences. (A) phage TP901-1 *vs* PhiLC3. Residues involved in receptor binding are identified by red dots. **(B)** Tuc2009 *vs* Q33.



Supplementary Figure S4 Structure and activation of phage p2 baseplate.. **(A)** The interaction between p2 Dit arm & hand domain and the RBP shoulders domain viewed from below the baseplate. **(B)** Structure of the p2 baseplate (Dit, Tal, RBP) viewed from above. **(C)** Lateral view of the p2 baseplate. **(D)** Structure of the p2 baseplate viewed from below. **(E)** Lateral view of the phage p2 activated baseplate. The RBPs have rotate 220° from the resting state.



Supplementary Figure S5. Hydrogen bonds established between phage PhiLC3 RBP N-termini and the Dit arm and hand domain.

Hydrogen bonds					
RBP			dist; (Å)	Dit hand	
1	B:TYR	17[N]	2.84	E:LEU	160[O]
2	B:ASP	10[N]	2.70	E:PHE	162[O]
3	B:LEU	16[O]	3.36	E:ASN	158[ND2]
4	B:TYR	17[O]	3.66	E:LYS	159[N]
5	B:TYR	17[O]	3.29	E:LEU	160[N]
6	B:ASN	97[OD1]	3.32	E:THR	288[OG1]
1	C:TYR	17[N]	2.83	E:LEU	164[O]
2	C:ASP	10[N]	2.74	E:ILE	166[O]
3	C:TYR	17[O]	2.50	E:LEU	164[N]
4	C:ASP	10[OD2]	2.95	E:SER	165[OG]
1	D:ASP	10[N]	2.69	E:ALA	173[O]
2	D:TYR	17[N]	2.87	E:PHE	170[O]
3	D:ASN	9[OD1]	3.64	E:ALA	173[N]
4	D:ASP	10[O]	2.84	E:ILE	175[N]

Supplementary Figure S6. Buried surface area per residue between PhiLC3 RBP N-termini and the Dit arm and hand domain.

<div> <div> <div></div> <div>Inaccessible residues</div> </div> <div> <div></div> <div>Solvent-accessible residues</div> </div> </div> <div> <div>BSA</div> <div>Buried Surface Area, Å²</div> </div>					<div> <div> <div></div> <div>Residues making Hydrogen/Disulphide bond, Salt bridge or Covalent link</div> </div> <div> <div></div> <div>Interfacing residues</div> </div> </div> <div> <div>ΔG</div> <div>Solvation energy effect, kcal/mol</div> </div> <div> <div> </div> <div>Buried area percentage, one bar per 10%</div> </div>				
RBP	HSDC	ASA	BSA	ΔG	Dit hand domain	HSDC	ASA	BSA	ΔG
B:PHE 6		54.57	16.80	0.27	E:ASN 148		112.42	13.12	-0.15
B:PRO 7		86.63	18.48	0.30	E:LYS 149		89.05	0.17	0.00
B:TRP 8		127.73	8.07	-0.03	E:SER 150		73.22	33.11	0.25
B:ASN 9		134.70	31.94	-0.14	E:ASN 156		102.09	16.13	-0.17
B:ASP 10	H	70.19	43.47	0.03	E:ASP 157		81.13	3.79	-0.04
B:ARG 15		91.47	3.80	-0.04	E:ASN 158	H	118.79	76.50	-0.12
B:LEU 16	H	145.68	79.52	0.98	E:LYS 159	H	103.80	3.37	0.05
B:TYR 17	H	79.47	68.09	0.18	E:LEU 160	H	72.67	67.47	0.50
B:ASP 18		86.82	64.89	0.41	E:LYS 161		146.29	52.58	0.72
B:ALA 19		65.57	20.34	0.21	E:PHE 162	H	160.99	92.39	0.82
B:ASP 20		79.65	1.72	-0.03	E:PRO 163		127.83	12.63	0.18
B:ASP 21		19.41	1.84	-0.02	E:PHE 172		136.44	54.23	0.80
B:PHE 22		111.27	30.42	0.48	E:ALA 173		37.39	8.62	0.14
					E:PHE 162		160.99	68.60	1.10
C:PHE 6		50.43	10.90	0.17	E:PRO 163		127.83	46.93	0.70
C:PRO 7		86.86	13.41	0.21	E:LEU 164	H	67.21	52.31	0.02
C:TRP 8		132.23	7.89	-0.04	E:SER 165	H	70.69	39.34	0.26
C:ASN 9		137.10	44.63	-0.20	E:ILE 166	H	136.35	82.45	0.63
C:ASP 10	H	73.83	61.79	-0.18	E:LYS 167		134.05	31.91	0.51
C:ARG 15		84.96	3.08	-0.04	E:THR 168		156.10	15.05	0.22
C:LEU 16		151.50	43.66	0.70					
C:TYR 17	H	74.31	65.39	0.18	E:ILE 166		136.35	53.91	0.86
C:ASP 18		83.95	20.35	0.27	E:LYS 167		134.05	5.89	-0.02
C:ALA 19		65.39	22.45	0.24	E:THR 168		156.10	44.55	0.11
C:PHE 22		106.82	28.12	0.45	E:ASP 169		114.37	27.52	0.29
					E:PHE 170	H	62.88	46.37	0.08
D:PHE 6		41.25	4.34	0.07	E:ALA 171		42.29	32.07	0.51
D:PRO 7		84.51	17.81	0.29	E:PHE 172		136.44	82.22	1.25
D:TRP 8		125.35	7.74	-0.04	E:ALA 173	H	37.39	28.78	0.00
D:ASN 9	H	136.85	78.68	-0.21	E:THR 174		64.10	28.30	0.38
D:ASP 10	H	68.16	60.18	-0.19	E:ILE 175	H	80.62	51.25	0.54
D:VAL 11		94.11	73.87	1.18	E:PRO 177		33.03	13.06	0.21
D:HIS 12		184.08	77.80	-0.25					
D:ASP 14		100.17	3.79	-0.06					
D:ARG 15		98.66	5.22	-0.06					
D:LEU 16		139.46	63.08	1.01					
D:TYR 17	H	70.54	60.08	0.05					
D:ASP 18		83.06	35.46	0.44					
D:ALA 19		63.37	17.40	0.18					
D:PHE 22		103.67	59.97	0.96					

Supplementary Figure S7. Comparison of the structural models of the adhesion devices with nsEM images. The nsEM images are reproduced in part from Figures 1 in references [2] and [3].

